

Microtremor Measurements for Regional Spatial Planning Based on Seismic Considerations in the Western Mataram City, West Nusa Tenggara Province, Indonesia

Siti Faridah¹, Urip Nurwijayanto Prabowo², Marjiyono³, Sismanto^{1,*}

¹Geophysics Laboratory, Department of Physics, Faculty of Mathematics and Natural Science, Gadjah Mada University, Sekip Utara, Bulaksumur, Yogyakarta 55281, Indonesia

²Department of Physics, Faculty of Mathematics and Natural Science, Universitas Jenderal Soedirman, Jl. Dr Soeparno No 6, Purwokerto, 53123, Indonesia

³Geological Survey Center, Geological Agency of the Ministry of Energy and Mineral Resources, Jl. Diponegoro No.57, Bandung, West Java, Indonesia

*Author to whom correspondence should be addressed:

E-mail: sismanto@ugm.ac.id

(Received May 22, 2025; Revised August 21, 2025; Accepted September 13, 2025)

Abstract: The Lombok earthquake on August 5, 2018, which originated from the back-arc thrust zone in the northern part of Lombok Island, caused extensive damage and casualties in Mataram City, the capital of West Nusa Tenggara Province, Indonesia. Therefore, disaster mitigation is essential to anticipate the impacts of future earthquakes, for example, by constructing major public facilities in zones with lower seismic vulnerability. This research aimed to assess seismic considerations in the western part of Mataram for regional spatial planning based on amplification value, peak ground acceleration (PGA), ground shear strain, and sedimentary layer thickness. We combined these parameters using the Simple Additive Weight (SAW) method to decide the potential area of high earthquake impact / seismic vulnerability. Microtremor data from 125 points in the western part of Mataram city were processed using the Horizontal to Vertical Spectral Ratio (HVSr) and Ellipticity Curve methods. The results show that the western part of Mataram has amplification factor values ranging from 2.610 to 10.590, PGA values ranging from 23.641 to 27.225 gal, ground shear strain ranging from 0.001 to 0.004, and sediment layer thickness ranging from 19 to 47 m. Sekarbela, Ampenan, and the southern part of Mataram exhibit the highest amplification factors, seismic vulnerability indices, and ground shear strain values. The results of the Simple Additive Weighting (SAW) method further indicate that these areas fall within the high seismic vulnerability zone. Based on the Indonesian National Standard (SNI) 1726-2019 which addresses earthquake-resistant design for building and non-building structures, we recommend that only structures in Risk Categories I and II be developed in these high seismic vulnerability (SV) zones. In contrast, for Selaparang subdistrict, which fall within the medium seismic vulnerability zone, we recommend the development of buildings classified under Risk Category III.

Keywords: ellipticity curve; HVSr; Mataram city; microtremor; risk categories

1. Introduction

Indonesia is a highly active tectonic region located near the boundaries of the Eurasia, Australia, Pacific and Philippine tectonic plates¹). The Indo-Australian plate subducts beneath the Eurasian plate, leading to a chain of volcanoes, including those in Sumatra, Java, Bali, and Lombok¹). This subduction process also results in high seismic activity in Indonesia²). Large earthquakes can cause significant loss of life and material damage. One of the largest earthquakes

in Indonesia was the Lombok earthquake on August 5, 2018, which originated from the back-arc thrust zone in the northern part of Lombok³). This earthquake caused extensive damage and casualties, including in Mataram City (Figure 1). Mataram city is the capital of West Nusa Tenggara Province, Indonesia. According to the building damage map of Mataram City, this earthquake damaged 21.66% of buildings in Sekarbela subdistrict, 19.76% in Ampenan subdistrict, 8.75% in Mataram and Selaparang subdistricts, 1.7% in Cakranegara subdistrict, and 7.76%

in Sandubaya subdistrict⁴). Mataram City, being the capital of West Nusa Tenggara, is a center of government, education, and trade with a high population density. Disaster mitigation is crucial in Mataram City to anticipate the impacts of future earthquake disasters, for example, by constructing major public facilities in safer zones with lower seismic vulnerability.

Numerous researchers have employed microtremor measurements to map seismic vulnerability zones, which serve as critical inputs for disaster mitigation strategies based on seismic risk assessment. Microtremors are ground surface vibrations originating from passive sources such as wind and sea waves⁵). The microtremor data describe the dynamic characteristics of the sedimentary layer/soil based on dominant periods and amplification factors using the Horizontal to Vertical Spectral Ratio (*HVSR*) method^{6,7}). These values can be used to obtain the seismic vulnerability index (*Kg*) and ground shear strain (*GSS* or γ) value. The *HVSR* curve, resulting from the *HVSR* method, can be used to determine the surface wave velocity (*Vs*) profile using the ellipticity curve method⁸). The *Vs* profile provides insights into the thickness of sedimentary layers⁹).

Gurler et al.¹⁰) utilized microtremor data to evaluate local site effects and estimate potential damage distribution in anticipation of earthquakes in Mexico City. Widyawarman et al.¹¹) mapped seismic vulnerability in Kebumen, Indonesia, using a vulnerability index derived from microtremor analysis. Similarly, Prabowo et al.¹²) applied microtremor measurements to identify landslide-prone areas in Kulon Progo, Indonesia, while Stanko et al.¹³) used similar techniques to delineate seismically hazardous zones in Ivanec, Croatia.

In addition to standalone microtremor analysis, some studies have integrated microtremor-derived parameters with other geophysical and environmental variables for more robust disaster risk assessment. Hadi et al.¹⁴) employed microtremor data to estimate peak ground acceleration (*PGA*), Modified Mercalli Intensity (*MMI*), seismic vulnerability index (*Kg*), shear wave velocity (*Vs*), and the average shear wave velocity in the top 30 meters (*Vs30*), which were then used to map seismic vulnerability in Bengkulu, Indonesia. Leonita et al.¹⁵) combined microtremor-derived parameters (the amplification factor and ground shear strain) with bedrock slope and *PGA* to identify fissure-prone zones in Demak, Indonesia, using the Simple Additive Weighting (*SAW*) method. Furthermore, Hadi et al.¹⁶) integrated microtremor-based parameters with fault distance, rainfall, slope, elevation, and land cover data using the Analytical Hierarchy Process (*AHP*) to assess landslide vulnerability zones.

Seismic vulnerability map is essential for supporting development planning in densely populated and urban areas with a high earthquake risk potential¹⁷). In this study, microtremor data acquired in 2013 were used to map the

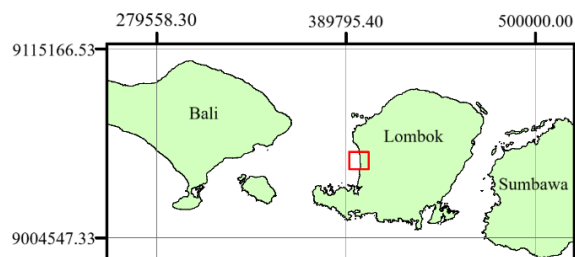


Fig. 1: Mataram, Lombok. Nusa Tenggara Barat. The red box indicates the area of this study

seismic vulnerability zones in the western part of Mataram. These maps were then compared with the building damage maps from the 2018 earthquake to validate the results against actual conditions. If the maps are proven to be valid, they can be correlated with SNI 1726:2019 to provide recommendations on the appropriate utilization of development facilities and to serve as a reference for regional spatial planning.

The study area includes the western part of Mataram City, encompassing the Ampenan, Selaparang, Sekarbela, and Mataram subdistricts, which experienced the highest building damage due to the earthquake.

The seismic vulnerability map combines amplification, sedimentary layer thickness, *PGA*, and γ from microtremor data analysis based on the Simple Additive Weight (*SAW*) method. The *SAW* method addresses multi-criteria or multi-attribute decision-making problems. Multicriteria decision analysis is an approach to decision-making that includes the assessment, prioritization, and selection of criteria (attributes) from different alternatives¹⁸). This research provides better information about the seismic vulnerability potential in the western part of Mataram City, serving as an essential reference in regional spatial planning. Spatial planning and infrastructure construction that consider seismic vulnerability based on microtremor data are crucial to reduce casualties and mitigate future earthquakes disaster^{11,14,19}).

2. Materials and Methods

The microtremor data was collected by the Geological Survey Center (*PSG*) in 2013, comprising 125 data points as shown in Figure 2. Each data point was measured over a duration of approximately 30 minutes. We analyzed the microtremor data using the Horizontal to Vertical Spectral Ratio (*HVSR*) method with Geopsy software. The *HVSR* method compares the horizontal wave spectral values in the east-west (*A_{EW}*) and north-south (*A_{NS}*) components with the vertical wave spectral values (*A_Z*) to obtain the *HVSR* curve using the following equation:

$$HVSR = \frac{S_{HS}}{S_{VS}} = \sqrt{\frac{(A_{NS})^2 - (A_{EW})^2}{A_Z}} \quad (1)$$

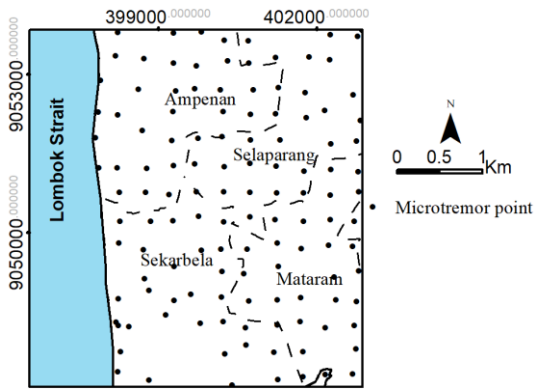


Fig. 2: Microtremor measurement points distribution

where S_{HS} is the spectrum of the horizontal component, and S_{VS} is the spectrum of the vertical component⁷⁾. The physical parameters derived from the *HVSR* curve are the dominant frequency value (f_0) and the ground amplification factor (A_0) due to earthquakes. These parameters are fundamental inputs for obtaining the seismic vulnerability index and ground shear strain. The seismic vulnerability index (Kg) is an index value that describes the level of vulnerability of sedimentary layers during an earthquake. Areas with low Kg values will have a relatively low potential for damage compared to areas with high values. Kg is calculated using the following equation⁶⁾

$$Kg = \frac{A_0^2}{f_0} \quad (2)$$

Ground shear strain (γ) is the maximum strain experienced by the surface soil during an earthquake. The ground shear strain is calculated using the following equation²⁰⁾

$$\gamma = e \frac{a_b}{\pi^2 V_{sb}} Kg \quad (3)$$

where a_b is the peak ground acceleration value on the bedrock, e is the efficiency of soil dynamic force, which is assumed 60%, and V_{sb} is the shear wave velocity value in the bedrock layer which is assumed 750 m/s based on SNI 1726: 2019 and array microtremor measurement in Mataram by Marjiyono²¹⁾. The ground shear strain (γ) values describe the soil condition when an earthquake occurs. When $\gamma > 1000 \times 10^{-6}$, the ground begins to show non-linear characteristics and when $\gamma > 10000 \times 10^{-6}$ large deformation and collapse occur^{20,22)}.

The peak ground acceleration value on the bedrock in the study area was determined using the Fukushima and Tanaka method²³⁾ based on an earthquake event that occurred on August 6, 2018, at coordinates -8.36670 latitude, 116.30620 longitude, with a depth of 10 km, and a magnitude (M_w) of 5.3²⁴⁾. The *PGA* is calculated using the following equation,

$$\log a_b = 1.3 + 0.41M - \log(R + 0.32 \times 10^{0.41M}) - 0.0034R \quad (4)$$

where a_b is the *PGA* value, M is the earthquake magnitude (M_w) and R is the hypocenter distance.

We use the *HVSR* curves to calculate the sediment layer thickness (h) based on the ellipticity curve method using a sub-program called *Dinver* in *Geopsy* software. The Ellipticity Curve is an inverse modeling method based on *HVSR* curve fitting²⁵⁾. The assumption used in this method is that surface waves dominate the microtremor data, and the H/V curve is dominated by the ellipticity of Rayleigh waves^{26,27)}. In this method, data fitting is performed to find model parameters that match the observation data (*HVSR* curve) to extract the surface shear wave velocity (V_s), as the function of depth^{27,28)}.

The seismic vulnerability map is generated to assess the seismic considerations for Regional Spatial Planning in the study area by combining the amplification, peak ground acceleration, ground shear strain, and sedimentary layer thickness using the Simple Additive Weight (*SAW*) method. The *SAW* values of the parameters and the corresponding weights assigned to each parameter are detailed in Table 1. The *SAW* values calculated using the following equation¹⁸⁾

$$A_j = \sum_{j=1}^n w_j x_{ij} \quad (5)$$

where A_j is the total score of the decision, x_{ij} is the ranking value of the i -th alternative in the j -th attribute and w_j is the weight value of j -th attribute. In Table 1, the amplification alternative is determined based on¹⁸⁾, the *PGA* alternative is determined based on BNPB Regulatory Chief No. 2 of 2012, the ground shear strain alternative is determined based on²⁹⁾ and the sedimentary layer thickness

Table 1: Weight normalization and standardization of alternative ranking score

Attribute	Weight Value (Normalization)	Alternative	Ranking
Amplification	0.34615	>9	5
		6-9	4
		3-6	3
		<3	2
Peak Ground Acceleration	0.30769	>0.70 g	5
		0.25-0.70 g	3
		<0.25 g	1
Ground Shear Strain	0.19231	>10 ⁻²	5
		10 ⁻³ - 10 ⁻²	3
		<10 ⁻³	1
Sedimentary layer thickness	0.15385	>50 m	5
		20-50 m	3
		<20 m	1

Table 2: Risk Categories and Types of Utilization of Development Facilities According to SNI 1726 - 2019

Type of Utilization	Risk Category
Buildings and non-building structures that pose low risk to human life in the event of failure include, but are not limited to, the following: Agricultural, plantation, livestock, and fishery facilities, temporary structures, storage warehouses, guard houses and other small-scale structures	I
All buildings and other structures not classified under Risk Categories I, III, or IV, including but not limited to: residential housing, shophouses and office houses, markets, office buildings, apartment buildings/condominiums, shopping centers/malls, industrial buildings, manufacturing facilities, factories	II
Buildings and non-building structures that pose a high risk to human life in the event of failure, including but not limited to: cinemas, convention halls, stadiums, healthcare facilities without surgical or emergency units, childcare facilities, correctional facilities (prisons), elderly care facilities Buildings and non-building structures, excluding those classified under Risk Category IV, that have the potential to cause significant economic impact and/or widespread disruption to daily public life in the event of failure, including but not limited to: conventional power plants, water treatment facilities, waste treatment facilities, telecommunication centers Buildings and non-building structures not classified under Risk Category IV (including, but not limited to, facilities for the manufacture, processing, handling, storage, use, or disposal of hazardous fuels, chemicals, wastes, or explosive materials) that contain toxic or explosive substances in quantities exceeding the threshold limits set by the competent authorities, and which pose a significant risk to the public in the event of a release.	III
Buildings and non-building structures classified as essential facilities, including but not limited to: monumental buildings, schools and educational facilities, places of worship, hospitals and other healthcare facilities equipped with surgical and emergency units, fire stations, ambulance services, police stations, and emergency vehicle garages, shelters for earthquakes, tsunamis, hurricanes, and other emergency refuge facilities, emergency preparedness centers, communication hubs, operations centers, and other emergency response facilities, power generation plants and other public utilities required during emergency situations, ancillary structures (including telecommunication towers, fuel storage tanks, cooling towers, substation structures, fire water tanks, or other buildings or support structures for	IV

water, materials, or firefighting equipment) that are required to remain operational during emergencies	
---	--

Table 3: The correlation of *SAW* total score and seismic vulnerability decision with the SNI 1726: 2019 to make a recommendation of building type and utilization

<i>SAW</i> Value	Seismic vulnerability Category	Recommendation of building Risk category
0.75 – 1	Very high	I
0.5 – 0.75	High	I and II
0.25 – 0.5	Medium	I, II, and III
0 – 0.25	Low	I, II, III, and IV

is divided based on the interval of the ellipticity curve results. The *SAW* total score and seismic vulnerability decision are correlated with the Risk Categories and Types of Utilization of Development Facilities According to SNI 1726: 2019 (Table 2) to make a recommendation of building type and utilization which not suffered when an earthquake occurs (Table 3).

3. Results and Discussion

The result of the HVSR method is the HVSR pectrum curve as shown in Figure 3 HVSR curve with a single peak spectrum (Figure 3.a) corresponds to the condition of a homogeneous surface layer with the underlying layer having a significant impedance difference³⁰. The HVSR spectrum curve can have two peaks (Figure 3.b) that are caused by the presence of two impedance contrasts of a thin layer and the structure of another deeper layer beneath it^{31,32}. The dominant frequency of microtremor measurements does not always show one-layer characteristics due to complex ground vibration movements. In cases where two peaks are present, the specific peak is selected based on the similarity of its dominant frequency to that of the nearest clear peak. Since the dominant frequency is proportional to the thickness of the sediment layer, nearby locations are expected to exhibit relatively similar dominant frequency values.

The dominant frequency values range from 0.373 Hz to 1.099 Hz (Figure 4). The low dominant frequency

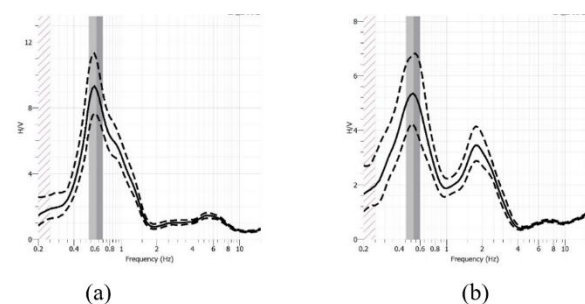


Fig. 3: (a) The one peak *HVSR* curve; (b) the two peaks *HVSR* curve

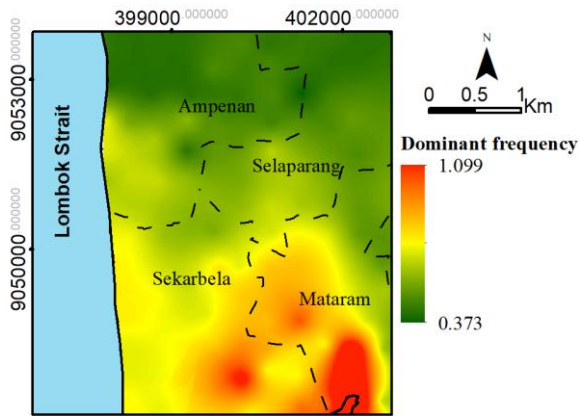


Fig. 4: The distribution of dominant frequency in the study area

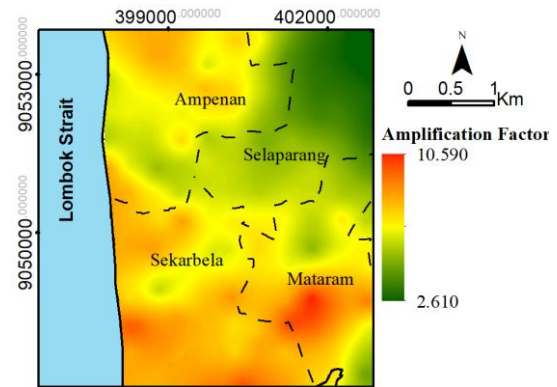


Fig. 5: The distribution of amplification factor in the study area

describes the thick surface sediment layer^{9,33,34}). Based on its geological formation³⁵), the study area is coastal area which has a soft sedimentary layer because it includes alluvial formations composed of shale, gravel, sand, clay, peat, and coral fragments. This reinforces previous research^{7,22,36}) which indicated that low frequency is associated with soft soil and thick sediment layer thickness. The lowest frequency is located on the north side including Ampenan and Selaparang subdistricts. The dominant frequency is a crucial parameter for earthquake disaster mitigation purposes, as it is related to earthquake-resistant building design. Structures with a natural frequency equal to the dominant frequency of the soil can experience resonance during an earthquake that potentially leads to rapid structural collapse during a strong earthquake. In addition to the dangers of earthquake vibration resonance, very low natural frequency values are vulnerable to long-period vibration hazards that can threaten high-rise buildings³⁷).

The amplification factor in Mataram City (Figure 5) range from 2.610 to 10.590 with the high values located in Sekarbela and Mataram Subdistricts. The highest amplification values are found along the western coastal area of the study region. The alluvial deposits in this coastal zone consist of loose sand with better sorting compared to the eastern area, resulting in higher impedance contrast and, consequently, greater seismic amplification²¹). A_0 refers to the phenomenon of increased amplitude or the degree of earthquake vibration when passing through specific soil layers^{6,38,39}). This means that the amplification factor can indicate how many times the soil will amplify the strength of an earthquake⁴⁰). The Sekarbela and Mataram subdistrict is more vulnerable to earthquake amplification than others because of its high amplification factor.

Based on the dominant frequency and amplification factor, we calculate the seismic Vulnerability Index (K_g) based on equation (4). The K_g values range from 16.945 to 171.742 (Figure 6). The higher K_g , the greater the vulnerability of

the surface soil to earthquakes, while the lower K_g , the lower the vulnerability of the surface soil. The high K_g dominates in Ampenan, Mataram, and Sekarbela subdistricts. A low K_g is observed in Selaparang subdistricts. The K_g value will be used to calculate ground shear strain.

Then we calculated the peak ground acceleration of the study area. PGA is the maximum or largest ground shaking acceleration value that occurs at the earthquake location and serves as a benchmark in seismic-resistant building design. This study shows the earthquake on August 6, 2018, resulted in the PGA value ranging from 23.641 to 27.225 gals. The distribution of PGA value (Figure 7) forms a diverse gradient pattern. The closer an area is to the epicenter, the higher its Peak Ground Acceleration (PGA) values, and vice versa. This is because PGA is influenced by both the earthquake's magnitude and the distance from the hypocenter. The distribution map indicates that Selaparang Subdistrict exhibits a high PGA value, which can be attributed to its proximity to the hypocenter located in the northeastern part of Lombok Island. The seismic event appears to have originated in the northwestern and northeastern regions of the island, characterized by medium to high levels of seismic activity⁴¹).

Based on PGA and K_g value, we calculated the ground shear strain on study area based on equation 3.

The γ can describe a material's ability to compress, stretch, and shear during an earthquake. A larger γ correlates with more susceptible soil layers to deformation. However, the small γ correlates with stable soil layers and is resistant to deformation. The γ values in the study area range from 0.001 to 0.004 (Figure 8). The high γ values observed in the Ampenan and Sekarbela subdistricts (along the western coastal area) are attributed to the coastal alluvial deposits characteristic of this region. The high γ is higher than 10-3 so it has elastic-plastic dynamic properties and is vulnerable to cracking to subsidence due to settlement when an earthquake occurs. There are no areas with γ values more than 10-2, so the study area is not vulnerable to liquefaction due to the earthquake.

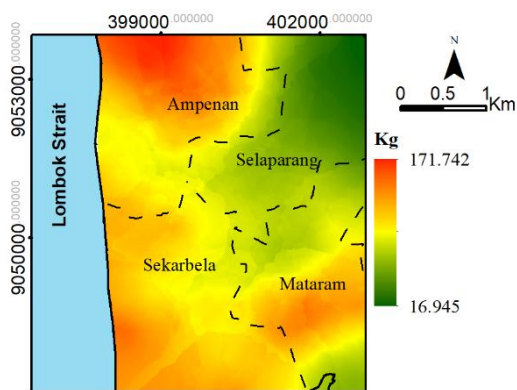


Fig. 6: The distribution of seismic Vulnerability Index (Kg)

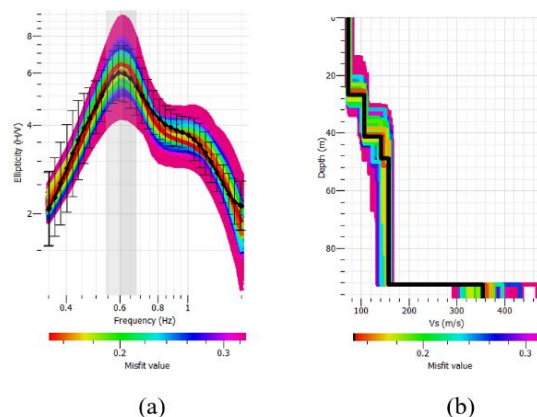


Fig. 9: (a) Ellipticity curve (b) V_s -depth profile

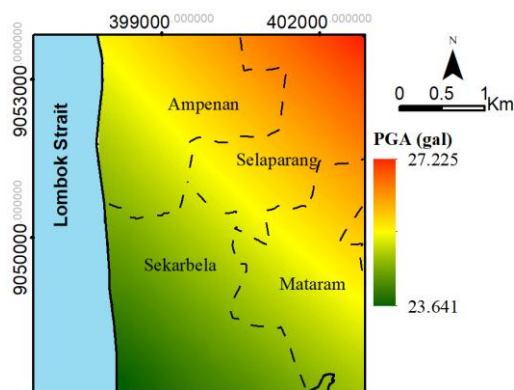


Fig. 7: PGA distribution in the study area

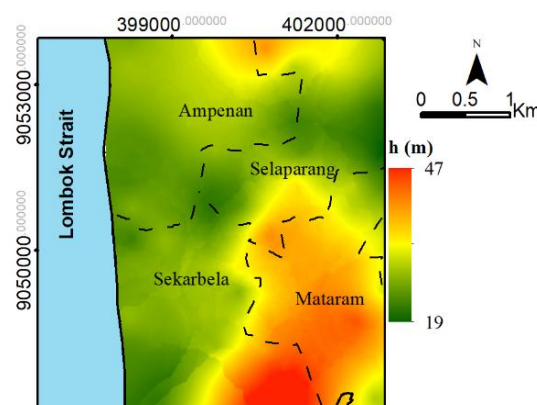


Fig. 10: Sedimentary layer thickness (h) distribution

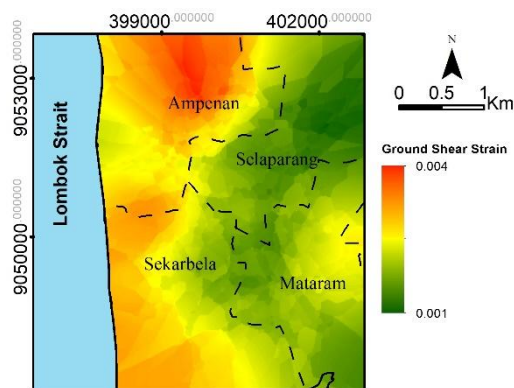


Fig. 8: Ground Shear Strain distribution

The sedimentary layer thickness is determined based on depth profile of soil (Figure 9b) resulted from the ellipticity curve (Figure 9.a)^{28,42}. We used the Dinver sub-program of Geopsy, with 1000 iterations to obtain the minimum error which indicates the resulting model closely approximates the actual conditions. We analyzed 125 microtremor data using the ellipticity curve method but only 63 data with low misfit (less than 0.35) were used to determine the depth profile. The sedimentary layer thickness is based on depth profile of soil ranges from 19 to 47 m (Figure 10). High sediment layer thickness values are located in the Sekarbela and Mataram subdistricts. The sediment layer in the study area primarily consists of alluvial deposits with sandy material. The thickness of soil

is widely used as a representation of subsurface structure of the region^{15,25,43} and local site affect^{10,12} that is crucial for identifying associated hazards and risks.

The seismic vulnerability (SV) in the study area is determined based on the Simple Additive Weight (SAW) results shown in Figure 11. The Ampenan, Sekarbela, and Mataram subdistricts are dominated by high SV classification which reflects the high earthquake-vulnerable areas. The 2018 earthquake damage map⁴ exhibits a pattern consistent with the Seismic Vulnerability (SV) map in this study, where the most severe damage occurred in the Ampenan and Sekarbela areas. Although the Mataram subdistrict did not experience significant damage during the 2018 earthquake, the SV map indicates a high potential for seismic vulnerability. This suggests that the structural strength and condition of buildings in the Mataram subdistrict need further investigation. The SV map reflects the seismic vulnerability of the near-surface sedimentary layers, which directly affect the overlying structures. However, if the buildings are well-constructed and earthquake-resistant, the potential damage caused by seismic events can be significantly reduced.

Based on Table 3, we recommended that building risk categories I and II to developed in this area and further research needs to be conducted when another building risk category will develop, especially the important facilities. The Selaparang subdistrict is dominated by a medium SV

Table 4: The seismic vulnerability values and recommendations of building risk category

Subdistrict	Lithology	Seismic Vulnerability classification	Recommendation of building Risk Category
Ampenan, Sekarbela	Alluvium	High	I, II
Mataram, Selaparang	Alluvium	High	I, II
		Medium	I, II, III

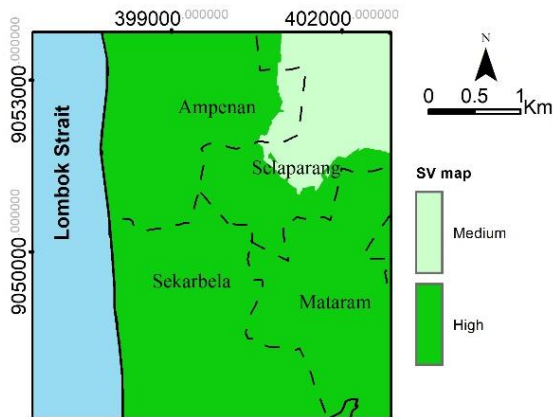


Fig. 11: Simple Additive Weight maps with Seismic Vulnerability classification.

classification with a high *SV* classification in a small area. So, we recommended the building risk categories I, II, and III mainly developed in Selaparang subdistricts. Table 4 shows the seismic vulnerability values and building recommendations for the western part of Mataram city, based on SNI 1726: 2019.

4. Conclusions

This study employed the Simple Additive Weighting (SAW) method to assess seismic vulnerability levels by integrating parameters such as amplification, peak ground acceleration (PGA), ground shear strain, and sedimentary layer thickness. These parameters reflect the geological and seismic characteristics of western Mataram City. The SAW analysis indicates that the subdistricts of Ampenan, Sekarbela, and Mataram exhibit high levels of seismic vulnerability. Therefore, it is recommended that only structures classified under Risk Categories I and II be developed in these areas. The findings of this study can serve as a reference for guiding development activities and enhancing earthquake-resilient planning efforts as part of broader earthquake disaster mitigation strategies in the western part of Mataram City.

Acknowledgements

We would like to express gratitude to the Geological Survey Center in Bandung for providing data for this study.

Nomenclature

- A_0 ground amplification factor (–)
- V_s surface shear wave velocity ($m \cdot s^{-1}$)
- f_0 dominant frequency (Hz)
- HVSR horizontal to vertical spectral ratio (–)
- K_g seismic vulnerability index (–)
- PGA peak ground acceleration (gals or $cm \cdot s^{-2}$)
- SAW simple additive weight (–)
- SV seismic vulnerability (–)

Greek symbols

- γ ground shear strain (–)

References

- 1) Y. Bock, L. Prawirodirdjo, J.F. Genrich, C.W. Stevens, R. McCaffrey, C. Subarya, S.S.O. Puntodewo, and E. Calais, “Crustal motion in Indonesia from global positioning system measurements,” *J Geophys Res Solid Earth.*, 108 (B8) 1-21 (2003). doi:10.1029/2001JB000324.
- 2) S.J. Hutchings, and W.D. Mooney, “The seismicity of Indonesia and tectonic implications,” *Geochemistry, Geophysics, Geosystems*, 22 (9) 1-42 (2021). doi:10.1029/2021GC009812.
- 3) R.M. Taruna, and G.K.S. Bunaga, “Ground motion database for Lombok-Sumbawa back arc thrust in 2007-2021 period,” *Seminar Nasional Fisika (SNF) 2021, Universitas Negeri Surabaya, Surabaya.*, 129–135 (2021)
- 4) B. Setyogroho, D. Muslim, M.S. Sadewo, G.O. Muslim, S. Burhanuddin, and H. Hendarmawan, “Correlation between building damages and losses with the microzonation map of Mataram—case study: Lombok earthquake 2018, Indonesia,” *Sustainability (Switzerland)*, 14 (4) 1-14 (2022). doi:10.3390/su14042028.
- 5) H. Okada, “The Microtremor Survey Method (Geophysical Monograph Series No. 12),” Society of Exploration Geophysicists, Tulsa, 2003. doi: 10.1190/1.9781560801740.fm
- 6) Y. Nakamura, “Clear Identification of Fundamental Idea Of Nakamura’S,” *Proc XII World Conf. Earthquake Engineering. Vol 24, New Zealand.*, 25-30 (2000).
- 7) Y. Nakamura, “A method for dynamic characteristics estimation of subsurface using microtremor on the ground surface,” *QR of RTRI*, 30 (1) 25–33 (1989).
- 8) R. Xu, and L. Wang, “The horizontal-to-vertical spectral ratio and its applications,” *EURASIP J Adv Signal Process*, 2021 (1) 1-10 (2021). doi:10.1186/s13634-021-00765-z.
- 9) M.I. Seht, and J. Wohlenberg, “Microtremor measurements used to map thickness of soft sediments,” *Bulletin of the Seismological Society of America*, 89 (1) 250–259 (1999). doi:

- 10.1785/BSSA0890010250.
- 10) E.D. Gurler, Y. Nakamura, J. Saita, and T. Sato, "Local site effect of Mexico City based on microtremor measurement," *Proceeding of 6th International Conference of Seismic Zonation*, (1990).
 - 11) D. Widyawarman, S. Sismanto, and A.Y. Purnama, "Mapping earthquake vulnerable areas based on microtremor measurements near Kebumen city," *Malaysian Journal of Science*, 43 (4) 38–43 (2024). doi:10.22452/mjs.vol43no4.5.
 - 12) U.N. Prabowo, A.F. Amalia, and F.E. Wiranata, "Local site effect of soil slope based on microtremor measurement in Samigaluh, Kulon Progo, Yogyakarta," *J Phys Conf Ser*, 1–7 (2018). doi: 10.1088/1742-6596/997/1/012007
 - 13) D. Stanko, S. Markušić, M. Gazdek, V. Sanković, and I. Slukan, "Assessment of The Seismic Site Amplification in the City of Ivanec (nw part of Croatia) using the microtremor hvsr method and equivalent-linear site response analysis," *Geoscience*, 9 (213) 1–25 (2019). doi:10.3390/geosciences9070312.
 - 14) A.I. Hadi, M. Farid, L.Z. Mase, R. Refrizon, S.B. Purba, D.I. Fadli, and E. Sumanjaya, "Zonation of seismic vulnerability levels in south Bengkulu regency, Indonesia for disaster-based regional planning," *Rudarsko-Geološko-Naftni Zbornik*, 39 (2) 133–148 (2024). doi:10.17794/rgn.2024.2.11.
 - 15) R. Leonita, S. Sismanto, and M. Marjiyono, "Microtremor analysis to identify fissure vulnerable zones in Demak, Central Java, Indonesia," *Sains Malaysiana*, 53 (7) 1533–1544 (2024). doi:10.17576/jsm-2024-5307-05.
 - 16) A.I. Hadi, M. Farid, L.Z. Mase, Refrizon, R. Mulyasari, M.A. Nabhan, D.I. Fadli, E. Putriani, and E. Sumanjaya, "Mapping landslide vulnerability using subsurface rock elastic parameters: a case study of Lebong regency, Bengkulu," *Kuwait Journal of Science*, 52 (2) 1-16 (2025). doi:10.1016/j.kjs.2025.100393.
 - 17) Ö. Yilmaz, "Engineering Seismology with Applications to Geotechnical Engineering," Society of Exploration Geophysicists, 2015. doi: 10.1190/1.9781560803300.fm
 - 18) J.J.H. Setiawan, "Mikrozonasi Seismisitas Daerah Yogyakarta dan Sekitarnya," Institut Teknologi Bandung, 2009.
 - 19) B. Harlianto, D.I. Fadli, E. Sumanjaya, A.I. Hadi, A. Maulidiyah, Suwarsono, and E.H. Purwanto, "Seismic vulnerability along the Kaur-South Oku highway in Bengkulu, Indonesia: planning for more resilient and safer cities," *Indian Geotechnical Journal*, 55 (5) 3042–3057 (2024). doi:10.1007/s40098-024-01101-6.
 - 20) Y. Nakamura, "Seismic Vulnerability Indices For Ground And Structures Using Microtremor," *World Congress on Railway Research, Florence*, 1-7 (1997).
 - 21) Marjiyono, "Configuration of quaternary basin in Mataram city area, West Nusa Tenggara based on microtremor data," *Jurnal Geologi Dan Sumberdaya Mineral*, 17 (1) 51–60 (2016). doi: 10.33332/jgsm.geologi.v17i1.29
 - 22) Y. Nakamura, T. Sato, and M. Nishinaga, "Local Site Effect Of Kobe Based On Microtremor," *Proceeding of the Sixth International Conference on Seismic Zonation EERI, Palm Springs California*, 3-8 (2000).
 - 23) T. Fukushima, Y. dan Tanaka, "A new attenuation relation for peak horizontal acceleration of strong earthquake ground motion in Japan," *Bulletin of the Seismological Society of America*, (80) 757–783 (1990). doi: 10.1785/BSSA0800040757
 - 24) USGS, "Earthquake catalog (1900-2023)," [Http://Earthquake.Usgs.Gov/Earthquakes/Eqarchive/s/Epic/Epic_rect.Php](http://Earthquake.Usgs.Gov/Earthquakes/Eqarchive/s/Epic/Epic_rect.Php), accessed August 2023.
 - 25) V.L. Ipmawan, I.N.P. Permanasari, and C. Suhendi, "Ambient noise-based mapping of bedrock morphology and potential fissure zone in East Tanjung Karang, Bandar Lampung, Lampung, Indonesia," *Makara Journal of Science*, 25 (2) 61–68 (2021). doi:10.7454/mss.v25i2.1205.
 - 26) D. Fäh, F. Kind, and D. Giardini, "Inversion of local s-wave velocity structures from average h/v ratios, and their use for the estimation of site-effects," *Journal of Seismology*, 7 449–467 (2003). doi: 10.1023/B:JOSE.0000005712.86058.42
 - 27) M. Wathelet, J. D., and M. Ohrnberger, "Surface-wave inversion using a direct search algorithm and its application to ambient vibration measurement," *Near Surface Geophysics*, 2 211–221 (2004). doi: 10.3997/1873-0604.2004018
 - 28) M. Hobiger, P.Y. Bard, C. Cornou, and N. Le Bihan, "Single station determination of Rayleigh wave ellipticity by using the random decrement technique," *Geophys Res Lett*, 36 (14) 1-5 (2009). doi: 10.1029/2009GL038863
 - 29) K. Ishihara, "Evaluation of Soil Properties for Use in Earthquake Response Analysis," *Proc. Int. Symp. On Numerical Model in Geomech*, (1982).
 - 30) Marjiyono, "Estimasi Karakteristik Dinamik Tanah Dari Data Mikrotremor Studi Kasus Wilayah Kota Bandung. Bandung," Thesis, Institut Teknologi Bandung, 2010.
 - 31) SESAME European Research Project, "Guidelines For The Implementation Of The H / V Spectral Ratio Technique On Ambient Vibrations Measurements , Processing And Interpretation," 2004.
 - 32) Z.L. Kyaw, S. Pramumijoyo, S. Husein, T.F. Fathani, and J. Kiyono, "Seismic Behaviors Estimation of the

- Shallow and Deep Soil Layers Using Microtremor Recording and EGF Technique in Yogyakarta City , Central Java Island,” *Procedia Earth and Planetary Science*, 31–46 (2015). doi:10.1016/j.proeps.2015.03.024.
- 33) Marjiyono, Ratdomopurbo, Suharna, Moch.H.H. Zajuli, and R. Setianegara, “Geologi bawah permukaan dataran klaten berdasarkan interpretasi data mikrotremor,” *Geologi Dan Sumberdaya Mineral*, 15 (1) 3–10 (2014). doi: 10.33332/jgsm.geologi.v15i1.66
- 34) U.N. Prabowo, A. Ferdiyan, and A.F. Amalia, “The soft layer thickness estimation using microtremor measurement to identify laandslide potential in watukumpul, central java, indonesia,” *Geoscience, Engineering, Environment and Technology*, 6 (1) 16–23 (2021). doi: 10.25299/jgeet.2021.6.1.5436
- 35) S.A. Mangga, S. Atmawinata, B. Hermanto, B. Setyonugroho, and T.C. Amin, “Peta Geologi Lembar Lombok, Nusatenggara Barat, skala 1:250.000,” Bandung, 1994.
- 36) S. Parolai, P.Bormann, and C. Milkereit, “New relationships between vs, thicknes of sediments, and resonance frequency calculated by the h/v ratio of seismic noise for the cologne area (germany),” *Bull of Seismological Society of America*, 92 (6) 2521–2527 (2002). doi: 10.1785/0120010248
- 37) R. Tuladhar, “Seismic Mikrozonation of Greater Bangkok Using Mikrotremor,” Thesis, Asian Institute of Technology, 2002.
- 38) Marjiyono, “Potensi penguatan gelombang gempabumi oleh sedimen permukaan kota mataram nusa tenggara barat,” *Jurnal Lingkungan Dan Bencana Geologi*, (2016).
- 39) U.N. Prabowo, Marjiyono, and Sismanto, “Amplifikasi dan atenuasi gelombang seismik di lapisan sedimen permukaan,” *Sciencetech*, 2 (1) 112–116 (2016). doi: 10.30738/jst.v2i1.414
- 40) P. Pornsopin, P. Pananont, K.P. Furlong, S. Chaila, C. Promsuk, C. Kamjudpai, and K. Phetkongsakul, “Seismic microzonation map of chiang mai basin, thailand,” *Trends in Sciences*, 21 (3) 1–13 (2024). doi:10.48048/tis.2024.7370.
- 41) D. S. Agustawijaya, H. Sulistiyono, and I. Elhuda, “Determination of the seismicity and peak ground acceleration for lombok island: an evaluation on tectonic setting,” *MATEC Web of Conferences*, 195 03018 (2018). doi:10.1051/mateconf/201819503018.
- 42) S. Castellaro, and F. Mulargia, “VS30 estimates using constrained h/v measurements,” *Bulletin of the Seismological Society of America*, 99 (2A) 761–773 (2009). doi:10.1785/0120080179.
- 43) S.Y. Kang, K.-H. Kim, J.-M. Chiu, and L. Liu, “Microtremor hvsr analysis of heterogeneous shallow sedimentary structures at pohang, south korea,” *Journal of Geophysics and Engineering*, 1–9 (2020). doi:10.1093/jge/gxaa035.